AMERICAN JOURNAL OF PHYSICAL ANTHROPOLOGY 109:211–227 (1999)

Effects of Loading on the Biochemical Behavior of Molars of *Homo*, *Pan*, and *Pongo*

GABRIELE A. MACHO* AND IAIN R. SPEARS
Hominid Palaeontology Research Group, Department of Human Anatomy and Cell Biology, University of Liverpool, Liverpool L69 3GE, UK

KEY WORDS mastication; molars; functional adaptation; finite element stress analyses; biomechanics; orofacial skeleton; *Pan*; *Pongo*

ABSTRACT In a previous study, we found systematic differences in the biomechanical behavior of modern human molars using finite element stress analyses (FESA), which led us to propose that molars are adapted to differently-directed loads depending on their position within the mouth (Spears and Macho [1998] Am. J. Phys. Anthropol. 106:467–482). While the FESA results thus derived have not been verified experimentally, such an interpretation seemed reasonable. To refine the model previously presented, this study assessed the effects of 1) food particle size on the biomechanical behavior of molars, and those of 2) differences in morphology, particularly enamel thickness, on stress distribution. In order to appraise the evolutionary significance of the findings, the FESA results for modern humans were subsequently compared with those obtained for molars of one individual of *Pan* and *Pongo*, respectively. Bearing in mind limitations imposed by the FESA models created and analyzed in this study, constant cleavage-type loads and cuspal tip loads at different directions were employed on all teeth: this facilitated comparisons of patterns of stress distribution across molars and species. In *Pan* and *Homo*, cleavage-type loads exerted by big food particles tended to be better dissipated anteriorly than posteriorly, although trends in *Pongo* were less clear-cut. Furthermore, similar to modern humans, the buccal cusps of mandibular molars appeared to be able to dissipate the loads associated with a pestle-type action, while maxillary molars were better designed to dissipate the loads which would result if they acted as mortars against which the food is crushed/ground. While increases in enamel thickness lowered the overall stress values in teeth only slightly, changes in outer morphology could have a more profound effect on these stress levels. Overall, *Pan* appeared to be most generalized, while *Homo* and *Pongo* showed a number of unique specializations, which are in accordance with what is currently understood about their respective masticatory apparatus and dietary niche. Am J Phys Anthropol 109:211–227, 1999.

Teeth, unlike other biological structures, are not amenable to direct mechanical experiments such as strain gauge evaluation. Yet, knowledge of the biomechanical behavior of teeth is essential for an understanding of the functional adaptations of the orofacial skeleton, and its evolutionary history. Finite element stress analysis (FESA), a math-

Grant sponsor: R.D.F., Liverpool University; Grant sponsor: N.E.R.C.; Grant number: GR9/01635; Grant sponsor: Leverhulme Trust; Grant number: F/25/BK.

Iain R. Spears is now at Sektion Biomechanik, TU Hamburg-Harburg, Harburger Schloßstr. 36, D-21079 Hamburg, Germany.

*Correspondence to: Gabriele A. Macho, Hominid Palaeontology Research Group, Department of Human Anatomy and Cell Biology, University of Liverpool, PO Box 147, Liverpool L69 3GE, UK. E-mail: gamal@liverpool.ac.uk

Received 14 April 1998; accepted 1 March 1999.

ematical modeling technique, affords the opportunity to predict stresses in biological structures such as teeth (Yettram et al., 1976; Rubin et al., 1983; Khera et al., 1988; Goel et al., 1990, 1991, 1992). This mathematical technique examines the deformations of a model composed of a meshwork of elements with given material properties, e.g., of enamel and dentine, under specific loads. Although a number of assumptions must be made in creating such models, FESA provides a powerful tool which has been successfully employed in the design of various restorations (e.g., Asaoka, 1994; Holmes et al., 1996) and in elucidating the biomechanical behavior of intact teeth (Yettram et al., 1976; Spears et al., 1993). In the present study, this technique will be employed to investigate the mechanical behavior of different molars from various species. Based on the assumption that teeth, like other structures of the body, are adapted to the loads they habitually undergo, the functional demands placed on a tooth may be inferred from its morphology.

In a previous paper, FESA models of isolated, unworn maxillary and mandibular modern human molars were created and subjected to differently-directed cleavage-type loads (Spears and Macho, 1998). The outward displacement of cusps caused by such loads has been implicated in the origins of cuspal fractures (Granath and Svensson, 1991; Panitvisai and Messer, 1995), and is thus considered useful in determining the range of loads which molars are adapted to. Systematic differences in morphology, especially enamel thickness (Macho and Berner, 1993, 1994), and in the biomechanical behavior of molars, led us to propose a specialized model of mastication: maxillary molars seem better suited to act as mortars against which the food is crushed/ground, whereas buccal cusps of mandibular molars are better suited to act as pestles (Spears and Macho, 1998). Owing to the functional constraints imposed by the orofacial skeleton, first maxillary molars should be able to resist loads directed at them at different angles and from different-sized food particles, while posterior molars could be more restricted in their biomechanical behavior but should be well-designed to dissipate loads resulting from relatively small objects being crushed onto their guiding cusps by near-vertical masticatory movements and high bite forces (Spears and Macho, 1998). These interpretations are reasonable, although it is acknowledged that the FESA results have not been verified experimentally, that a sound understanding of the underlying factors causing different high/low values of stress is still lacking, and that the evolutionary processes of stress adaptation in teeth are poorly understood. To refine the FESA model previously presented, this study will first assess the effects of food particle size on the biomechanical behavior of molars and will appraise the influence of morphology, i.e., enamel thickness, on stress distribution. Subsequently, we shall attempt to shed light on the evolutionary significance of the biomechanical patterns observed.

As regards the phylogenetic relationship of hominoids, *Pan* is most closely related to *Homo*, with *Gorilla* having branched off somewhat before (Kim and Takenaka, 1996; Ruvolo, 1997). The evolution and radiation of the *Pongo* clade occurred earlier (Mohammad-Ali et al., 1995), probably during the Middle Miocene (Moyà Solà and Köhler, 1993). Although many of the craniofacial traits in the orangutan are generally considered derived for the *Sivapithecus/Pongo* clade (Andrews, 1992), recent evidence suggests that *Pongo* might have retained the primitive condition of ancestral Hominoidea in many respects, especially in features of upper facial morphology (Benefit and McCrossin, 1997). Morphologically and behaviorally, *Pongo* is also distinct from the African apes (Andrews and Cronin, 1982; Fleagle, 1988). Like other hominoids, *Pongo* is predominantly frugivorous (MacKinnon, 1971, 1974), but it is unique in commonly preparing large, hard fruits with its incisors and exerting high bite forces with its postcanine teeth to crack open hard seeds (Lucas et al., 1994). An experimental study has shown that the magnitude of these bite forces may be close to 2,000 N (Lucas et al., 1994). Maximum bite forces in modern humans are below 1,000 N, as shown experimentally (Pruim et al., 1978) and theoreti-

cally (Koolstra et al., 1988; Osborn, 1996), while those in *Pan*, estimated from cranial morphology, appear to be between those of *Homo* and *Pongo* (Demes and Creel, 1988). Overall, the craniodental morphology of *Pan* is considered more generalized and shows similarities with *Homo* in many respects (Smith, 1986). There are, however, anatomical differences between the two species, which may be reflected in the biomechanical behavior of the molars. These are the length of the palate and its retraction beneath the skull (Rak, 1983) and, related to this, the markedly less pronounced axial inclination of posterior molar roots in *Pan* (Smith, 1986). This may affect the angle of approach of mandibular and maxillary molars during mastication (Spears and Macho, 1998). Also, chimpanzees (and other hominoids), unlike modern humans, retain the disparity in maxillary and mandibular arch widths (i.e., maxillary overjet) from anterior to posterior (Smith, 1986). Although mainly frugivorous, chimpanzees also regularly hunt and consume small animals (McGrew et al., 1996), and tend to use tools rather than teeth for opening hard objects such as nuts (Boesch and Boesch, 1990; McGrew, 1992). Given their evolutionary histories, as well as their morphological and behavioral (dis)similarities, analyses of *Pan* and *Pongo* molars (and *Homo*) are considered particularly useful for an appraisal of the possible evolutionary significance of the findings and may allow inferences to be made about hominoids in general, both extant and extinct. Comparative FESA on *Pan*, *Pongo*, and *Homo* molars will therefore be carried out.

The questions addressed in the present study can be summarized as follows: 1) What are the effects of food particle size on the biomechanical behavior of modern human molars? 2) What are the effects of enamel thickness on the biomechanical behavior of teeth? 3) Are the results obtained for modern human molars comparable with those obtained for other hominoids, specifically *Pan* and *Pongo*? 4) Are the differences in biomechancial behavior observed between hominoid species likely to reflect differences in morphology, dietary niche, and/or phyletic separation?

MATERIALS AND METHODS

Twenty-nine sections through the mesial cusps of unworn modern human molars were available ($M^1 = 5$, $M_1 = 5$; $M^2 = 6$, $M_2 = 4$; $M^3 = 5$, and $M_3 = 4$) (Spears and Macho, 1998). Courtesy of David Beynon, tracings of cross sections through the mesial cusps of all six right permanent molars of a *Pongo pygmaeus* specimen (Beynon et al., 1991) and one *Pan troglodytes* individual were also available for study. First molars in these great ape specimens showed only little wear and, hence, reconstructions of the profiles of tooth crowns were possible.

Tracings of the cross-sectional outlines of the enamel caps were scanned with SAC Grafbar (AUTOCAD, revision 12 Autodesk, Inc.) and, using AUTOCAD, the outer surface of the outline of each tooth was digitized with 100 regularly spaced nodes, while the dentino-enamel junction (DEJ) was digitised with 75 nodes (Spears and Macho, 1998). The coordinates of these nodes were read into the finite element program ANSYS, version 5.3 (Ansys, Inc.). Using node and element direct generation, a mesh of 800 plane strain four-noded elements was created to represent the enamel cap (Fig. 1). Small elements were assigned in the intercuspal region to allow accurate representation of the anticipated high-stress gradient. The diameter of the pit, where present, was modeled as constant (0.16 mm), and the elements around the fissure were arranged so that the angle between adjacent edges did not exceed 15° (Fig. 1). The area enclosed within the DEJ and the cervical margin was meshed using the automesh facility available in ANSYS. Again, four-noded elements were specified but, because of the irregular geometry, some three-noded elements were included (Fig. 1).

The problems of predicting the magnitudes of tensile stresses in intercuspal fissures have already been discussed in greater detail (Spears and Macho, 1998) but, to reiterate, the magnitudes predicted by the model are most likely overestimations of the values that would occur in vivo if real teeth were subjected to the loads used in this study. Given the method of data collection employed here (i.e., photographed sections),

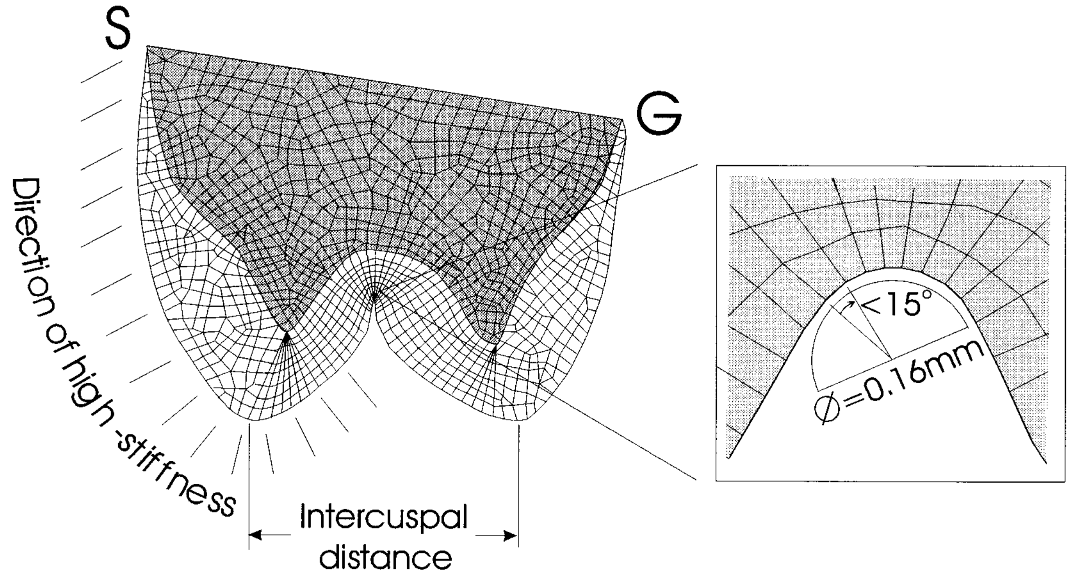

Fig. 1. Model of a maxillary second molar (M^2) of *Homo* showing the finite-element mesh created (S, supporting cusp; G, guiding cusp). Elements representing the standardized intercuspal fissure are shown.

it was not possible to differentiate between fissures of less than 0.16 mm in diameter. Notably, in a series of controlled tests in which the fissure diameter was varied, large differences in magnitudes of tensile stress were observed (Spears, unpublished findings): tensile stresses decreased when the diameter was increased, and vice versa. Bearing in mind the limitations of accurately modeling the intercuspal fissure and because this study was concerned with the effects of macromorphology on the stresses, it was considered justified to assume a constant radius. In order to obtain a truly realistic value of tension in the intercuspal region, microscopic data of the local three-dimensional structure, surface roughness, and chemical composition of enamel would have to be collected. Such data are not presently available.

As a consequence of its prismatic nature (Meckel et al., 1965), enamel is particularly weak under tension (Bowen and Rodriguez, 1962; Lee and Eakle, 1984, 1996), and the strength of the tooth under a given load will thus depend largely on its ability to minimize tensile stresses. In the present FESA models, the prismatic structure of enamel was considered and enamel was modeled to behave anisotropically with respect to stiffness (Spears et al., 1993). A Young's modulus of 90 GPa was assigned to represent the along-prism properties, whereas a value of 50 GPa was used to represent the across-prism properties of enamel. These values were predicted for enamel in which the volumetric proportion of mineralized tissue of enamel was 95% (Spears, 1997); although these values may be relatively high, they are nonetheless within the range of mature enamel. Over- or underestimation of the true mineral content of enamel would result in an over- or underestimation of tensile stresses, respectively, especially in the intercuspal region. Such systematic biases are considered unimportant for the present purpose, given that this study is concerned with detecting patterns of load dissipation between molars and species, and not actual instances of fracture. Prism direction is assumed to be perpendicular to the DEJ, and high stiffness was assigned accordingly (Fig. 1), although it is recognized that this is an oversimplification (Spears and Macho, 1998). Dentine was modeled as an isotropic material with a Young's modulus of 16.6 GPa (Waters, 1980). In the absence of data to suggest otherwise, Poisson's ratio of both

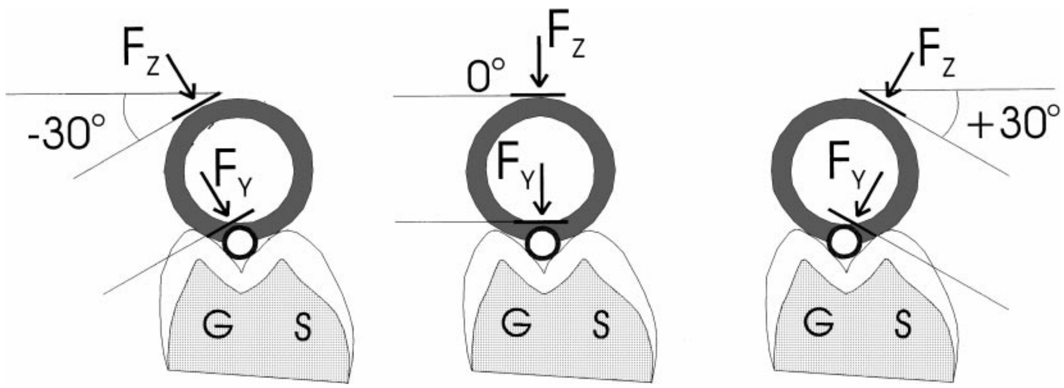

Fig. 2. The occlusal plane is considered a straight line joining the cusp tips, and the angle of loading is calculated accordingly. The angles at which the small (Y) and big (Z) food particle is loaded by the beam are shown. Constant loads of 1,000 N (F) are applied. S, supporting cusp; G, guiding cusp.

enamel and dentine was set at 0.3 (Waters, 1980). From these values, shear moduli were calculated automatically. Differences in size between molars were accounted for by scaling all teeth to the same bucco-lingual diameter (10 mm). Further description of the FESA models of teeth and their limitations can be found in Spears and Macho (1998).

A hollow food particle, with an outer diameter of one third of the respective intercusp tip distance of each tooth and an inner diameter of one fourth of the intercuspal distance, was modeled (Spears and Macho, 1998). In addition, a large circular food particle with a diameter of 6/9 of the intercuspal distance was modeled, while the inner diameter was scaled to 5/9 of the respective intercuspal distance. ANSYS Solid 42 elements with an assigned Young's modulus of 7.8 Gpa were created in order to represent the properties of *Mezzettia* seeds (Lucas et al., 1991), which are tough, strong, and stiff, and are known to be eaten by *Pongo* (Lucas et al., 1991, 1994), although not by the other species analyzed here. Since the aim of this study was the analysis of the biomechanical behavior of teeth under extreme conditions, rather than the prediction of the actual masticatory behavior of that species, the model of a *Mezzettia* was considered appropriate. Poisson's ratio of the seed was set at 0.3. The food particles were then placed onto the tooth model, and tooth-food contact was modeled. Frictionless contact was specified. Differences in the surface geometry of cusps previously led to difficulties when attempting to apply exactly the same load to the intercuspal surfaces (Spears, 1994). The decision to use contact elements, although increasing processing time, ensured that all teeth would undergo loads exerted by exactly the same food particle.

Instead of an opposing molar pushing the food particle into the occlusal basin, a long beam with an extremely high stiffness, which ensured negligible deformation during simulation, was used. The displacement of the beam was always in the direction perpendicular to its long axis (Fig. 2). The occlusal plane was defined as the straight line joining the cusp tips, and the lingual cusps were always kept to the left (Spears and Macho, 1998). Three loads were modelled: −30°, 0°, and +30°. When the beam model was held parallel to the defined occlusal plane, a value of 0° was assigned. Rotation of the beam towards positive angles always resulted in loads being predominantly exerted on the guiding cusps, whereas negative angles consistently loaded the supporting cusps (Fig. 2). Supporting cusps are those cusps which intercuspate with the occlusal basin of the opposing molar in central occlusion. Due to the mode of intercuspation in primates, lingual cusps of maxillary molars and buccal cusps of mandibular molars are thus considered supporting cusps.

In creating FESA models, simplifications are made. Notably, the three-dimensional structure of teeth is often modeled by using

a two-dimensional plane strain representation (Sakaguchi et al., 1992). The conditions of plane strain in which the out-of-plane strain is zero require that the modeled structure has constant cross-sectional geometry and is relatively long in the out-of-plane dimension (mesio-distally). Obviously, as regards teeth, these conditions are not met and in particular the intercuspal fissure is likely to disperse in a more mesial or distal section. However, it has been shown that the important features of tooth behavior can be represented by two-dimensional plane-strain elements (Sakaguchi et al., 1991) and, although in their study attention was not paid to fissure behavior, such elements are considered suitable for the present purposes. In the previous analysis (Spears and Macho, 1998), tensile stresses within the tooth were recorded at the instant at which the critical stress values in the food were reached. Direct comparison of stress levels between the two contacting bodies meant that the out-of-plane thickness of the tooth and food particle was inconsequential. However, for the purposes of this study in which comparisons of the behavior of teeth under the same load, but exerted via big and small food particles, were required, it was necessary to apply a standardized load. In the present study, the out-of-plane thickness, i.e., mesio-distal length, of the tooth models was therefore specified as 10 mm, and a standardized load of 10 N distributed along this length was applied to the food particles. Loads of 10 N were also applied to the cusp tips of both the guiding (negative values) and the supporting (positive values) cusp at a range of angles (Fig. 4), in order to test further whether one cusp may be particularly well-suited to dissipate load. This applied force is comparable with physiological bite-force values described by Delong and Douglas (1983). Given the range of foods eaten by a species, as well as the fact that the material properties of food changes during chewing, it is impossible to test the teeth during all loading conditions normally encountered by that tooth. However, with the exception of local variation in contact stress, the assumption of linear behavior for all materials modeled ensures that the general patterns of stress remain similar with higher (or lower) loads and stiffer (or more compliant) food properties. In addition, the shape of food particles would vary according to the stage of the chewing cycle or number of chews, gradually becoming more fragmented (if brittle) or more deformed (if tough). A further complication is that some materials can undergo a brittle-to-tough condition as the particle size is reduced. It is, therefore, acknowledged that the loading regimes exerted via the hollow food particles modeled here may only occur for a single instant during the period between ingestion and digestion. In this respect, the loads modeled could be considered similar to those exerted during puncture-crushing. Since the loads exerted during this stage of the chewing cycle are potentially the most damaging for the present purposes of interpreting molar morphology, an understanding of the behavior of teeth under these types of loads is the most appropriate. Statistical analyses were performed in Microsoft Excel (Version 6.0, Microsoft Corporation, Redmond, WA).

RESULTS

The maximum stresses in maxillary molars of *Homo* are given in Table 1 for small and big food particle loading, respectively. Descriptive statistics for mandibular modern human molars are given in Table 2. Trends shown in Tables 1 and 2 for small circular food particles are comparable to those presented previously (Spears and Macho, 1998; Tables 1 and 2 there), although there are differences in magnitudes of stresses owing to differences in research design, i.e., standardized loads (this study) instead of loads being applied until the point of food failure (previous study). While M^1s are well-suited to dissipate loads directed at them at different angles, i.e., towards buccal and lingual cusps, posterior maxillary molars are apparently better designed to dissipate loads exerted towards the guiding cusps (+30°) (Table 1). In mandibular molars, tensile stresses are consistently lower when the supporting cusps (-30°) are loaded (Table 2). These results are similar to those presented previously (Spears and Macho, 1998), although there are differences in overall trends when large circular food particles are

TABLE 1. Descriptive statistics of maximum principal stress (MPa) found in Homo maxillary molars when small (Y) and large (Z) circular food particles are pushed against the occlusal basin at different angles[1]

		−30° (supporting cusp)		0°		+30° (guiding cusp)		ANOVA	
Molar	N	Mean	SD	Mean	SD	Mean	SD	F-value	*P*
Small food particle loading (Y)									
M^1	5	1.50	0.39	1.98	0.74	1.42	0.56	1.34	0.298
M^2	6	2.91	0.97	2.96	1.03	1.22	0.40	8.12	0.004**
M^3	5	2.07	1.36	2.22	1.14	1.06	0.27	1.86	0.198
F-value		2.81		1.48		0.91			
P		0.097		0.264		0.430			
Big food particle loading (Z)									
M^1	5	1.56	0.52	1.34	0.32	1.09	0.26	1.87	0.195
M^2	6	2.89	0.90	2.52	0.53	1.94	0.35	3.43	0.059
M^3	5	3.04	0.82	2.72	0.49	1.86	0.42	5.06	0.025*
F-value		5.67		13.24		9.37			
P		0.017*		0.000***		0.003**			

[1] Results of analysis of variance (ANOVA) are also given between different angles of loading, as well as for differences between teeth at the same loading, for small (Y) and large (Z) food particle loading, respectively.
* $P < 0.05$.
** $P < 0.01$.
*** $P < 0.001$.

TABLE 2. Descriptive statistics of maximum principal stress (MPa) found in Homo mandibular molars when small (Y) and large (Z) circular food particles are pushed against the occlusal basin at different angles[1]

		−30° (supporting cusp)		0°		+30° (guiding cusp)		ANOVA	
Molar	N	Mean	SD	Mean	SD	Mean	SD	F-value	*P*
Small food particle loading (Y)									
M_1	5	1.02	0.70	2.18	1.47	2.30	1.24	1.78	0.209
M_2	4	1.39	0.47	2.47	0.75	2.44	0.74	3.46	0.076
M_3	4	1.00	0.20	1.96	0.45	2.05	0.54	7.61	0.012*
F-value		0.70		0.238		0.179			
P		0.521		0.790		0.838			
Big food particle loading (Z)									
M_1	5	1.45	0.84	2.62	1.36	2.75	1.27	1.83	0.203
M_2	4	1.55	0.38	2.26	1.06	2.58	1.69	0.80	0.477
M_3	4	1.10	0.47	1.77	0.70	2.27	0.97	2.49	0.138
F-value		0.59		0.65		0.14			
P		0.572		0.541		0.868			

[1] Results of analysis of variance (ANOVA) are also given between different angles of loading, as well as for differences between teeth at the same loading, for small (Y) and large (Z) food particle loading respectively.
* $P < 0.05$.

pushed against the occlusal basin (Tables 1 and 2).

First maxillary molars dissipate loads exerted by big food particles better than those exerted by small food particles when loads are directed away from the supporting cusp (Table 1). Compared with posterior upper molars, however, M^1s are well-designed to resist loads induced by big food particles, and all analyses of variance (ANOVAs) between teeth were statistically significant. Conversely, while guiding cusps (+30°) of posterior molars resist loads exerted by small circular food particles well, they appear poorly designed when big food particles are pushed against them (Table 1); nonetheless, stresses are still statistically significantly lower for guiding cusps (+30°) than for supporting cusps (-30°) or occlusal basins' (0°) loading (Table 1).

In mandibular molars, food particle size has apparently little effect on maximum principal stress, and loads exerted on the supporting cusps (-30°) are consistently better dissipated than those exerted on the guiding cusps (+30°), regardless of tooth position (Table 2). Hence, while food particle size appears to be important for trends in

TABLE 3. Paired t-tests between maximum stresses induced in Homo molars by big and small food particle loading at different angles[1]

Molars	−30° (supporting cusps) t-value	−30° (supporting cusps) *P*	0° t-value	0° *P*	+30° (guiding cusps) t-value	+30° (guiding cusps) *P*
M^1	0.17	0.87	−2.07	0.11	−1.91	0.13
M_1	2.28	0.08	0.85	0.44	0.76	0.49
M^2	−0.04	0.97	−0.92	0.40	2.57	0.05*
M_2	0.74	0.51	−0.49	0.65	0.18	0.87
M^3	1.63	0.18	0.90	0.42	4.69	0.01**
M_3	0.47	0.67	−0.50	0.65	0.35	0.75

[1] Negative t-values indicate that the tooth is better adapted to dissipate loads exerted by large food particles.
* $P < 0.05$.
** $P < 0.01$.

maximum stresses predicted in maxillary molars, the effects of size on mandibular molars seem negligible.

In order to shed further light on differences in the biomechanical behavior of teeth under small- and big-particle loading, paired t-tests were performed (Table 3). Statistically significant results were obtained for maxillary second and third molars only when the guiding cusp was loaded (+30°): guiding cusps of M^2s, and especially M^3s, are significantly better in dissipating small-particle loads (Table 3). Conversely, the relatively high (although not statistically significant) negative t-values for M^1s indicate that the occlusal basin (0°) and the guiding cusps (+30°) of these molars are better designed to dissipate loads resulting from large food particle loads.

Second and third maxillary molars in modern humans have relatively and absolutely thicker enamel than M^1s (Macho and Berner, 1993, 1994), and they also differ in outer morphology (Spears and Macho, 1995). In order to test the effects of enamel thickness on the biomechanical behavior of molars, two simple FESA models were created. Without changing the outer contour of the enamel cap, enamel thickness of a typical first molar was doubled while it was reduced by one half in an M^3 (Fig. 3). In both models, tensile stresses are consistently reduced by about 15% when the enamel is thick, i.e., in a thick-enameled M^1 and a normal M^3 (Fig. 3).

Comparable FESAs of food particle loadings were then carried out on molars of one *Pongo* and *Pan* specimen, respectively (Table 4). In *Pan*, few differences are observed between maxillary molars along the tooth row or between angles of approach when the small circular food particle is pushed against the tooth. When a large food particle is loaded, however, the supporting cusp dissipates the resulting loads more effectively than the occlusal basin (0°) or the guiding cusp (+30°). Mandibular molars of *Pan* are better at resisting loads exerted on the supporting cusp (-30°) than at the occlusal basin (0°) or the guiding cusp (+30°) (Table 4), and the superiority of supporting cusps in *Pan* is particularly marked when large food particles are loaded (Table 4).

In *Pongo*, both maxillary and mandibular molars dissipate loads better posteriorly than they do anteriorly, regardless of food particle size. This change in biomechanical behavior is particularly noticeable when big circular food particles are loaded. Moreover, although the supporting cusp (-30°) appears to be overall stronger than the guiding cusp (+30°) throughout the series, second and third maxillary molars slightly deviate from this trend when loads from big circular food particles are exerted: loading of the occlusal basin of M^2 and M^3 (0°) gave the lowest stress values (Table 4). Similar to *Homo* and *Pan*, loads directed onto the supporting cusps of mandibular molars are dissipated more effectively than loads directed towards the lingual cusps (Table 4).

Point loads on the cusp tips of guiding and supporting cusps further confirm the overall trends outlined above (Fig. 4). In modern humans, outwardly-directed loads on guiding cusps yield high tensile stresses in all mandibular molars, although high values are also obtained for M^2s and M^3s when point loads are applied to the cusp tips of supporting cusps. In *Pan*, guiding cusps of posterior mandibular molars appear particularly ineffective in load dissipation, while loads exerted elsewhere resulted in lesser levels of stress. Molars of *Pongo* are well-designed to resist high point loads, although loads exerted on the supporting cusps are marginally better dissipated than those exerted on the guiding cusps.

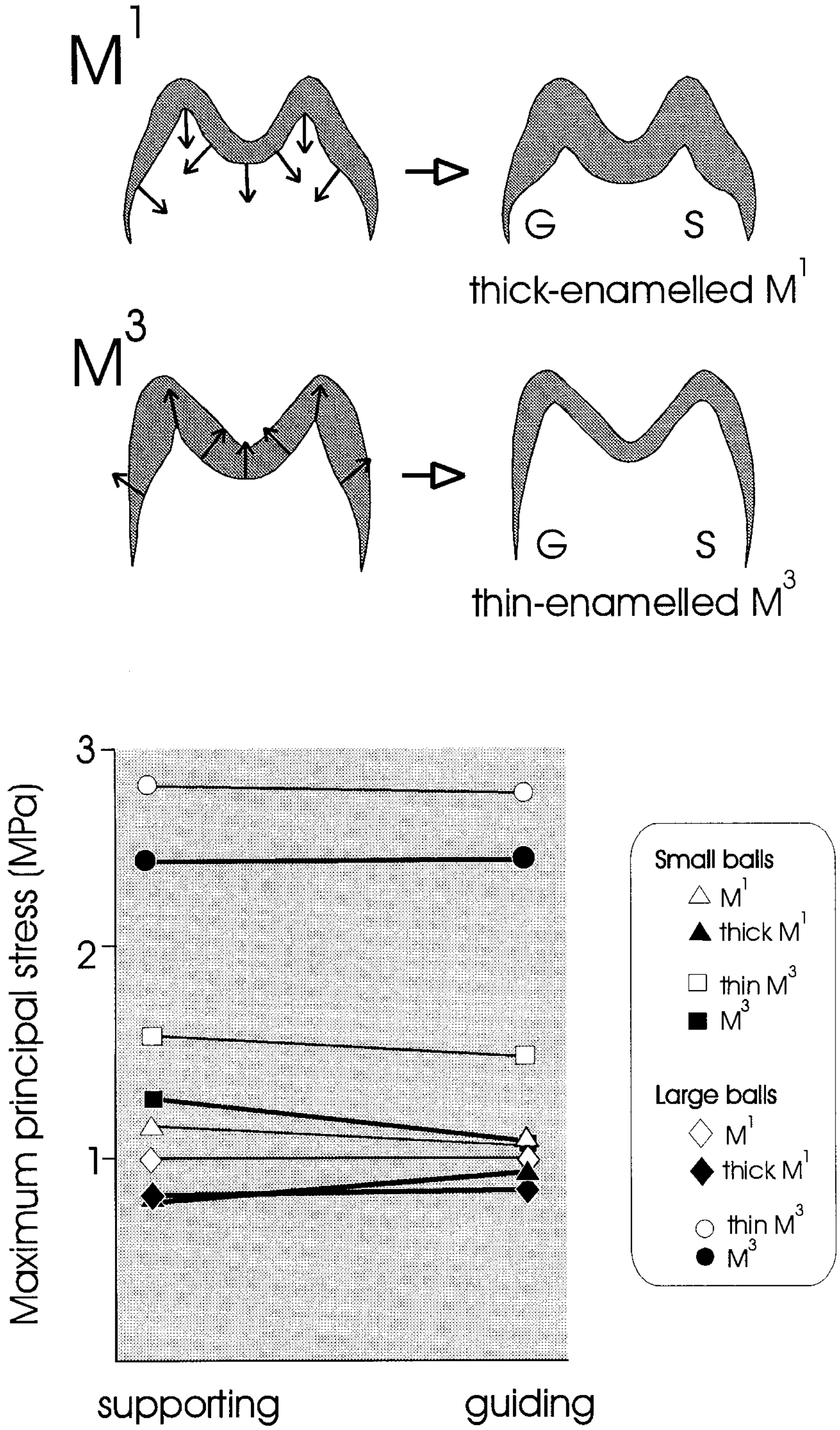

Fig. 3. In a typical first maxillary molar enamel thickness is doubled, whereas in a typical third maxillary molar it is halved; the outer contour of the enamel cap is kept constant. The results for small and big particle loading at ±30°, i.e., towards the supporting and the guiding cusp, respectively, are shown.

TABLE 4. Maximum stress (MPa) values for Pan and Pongo molars when small (Y) and large (Z) food particles are pushed onto the supporting cusp (−30°), guiding cusp (+30°), and both (0°)

	Pan			*Pongo*		
Molar	−30°	0°	+30°	−30°	0°	+30°
Small food particle loading (Y)						
M^1	0.55	0.63	0.52	0.60	1.84	1.51
M^2	0.60	0.62	0.59	0.48	0.55	0.64
M^3	0.57	0.60	0.58	0.37	0.50	0.60
M_1	0.97	1.49	1.24	0.69	1.21	1.04
M_2	0.64	0.50	1.20	0.52	0.60	0.61
M_3	0.43	0.82	1.83	0.35	0.41	0.70
Big food particle loading (Z)						
M^1	0.68	1.01	1.32	1.15	1.71	0.68
M^2	0.59	1.12	1.11	0.68	0.45	0.59
M^3	0.75	0.90	0.90	0.62	0.37	0.75
M_1	1.11	1.22	1.14	0.77	1.17	1.11
M_2	1.01	2.62	3.03	0.51	0.57	1.01
M_3	1.12	2.96	4.47	0.32	0.40	1.12

DISCUSSION

This investigation builds on, and extends, a previous study on modern human molars, which found systematic differences in the biomechanical behavior of isolated teeth (Spears and Macho, 1998). In accordance with the previous study, buccal cusps of mandibular molars are consistently stronger than guiding cusps, thus emphasizing their possible role as pestles during mastication (Table 1). As expected, first maxillary molars are well-adapted to dissipate loads regardless of food particle size and angle of approach, but M^2s and M^3s respond differently to loading of small and big circular food particles. Although the guiding cusps of these latter teeth are consistently better adapted to dissipate loads than the supporting cusps, the maximum principal stresses are markedly increased, both relatively and absolutely, when big food particles are simulated (Tables 1, 3). The difference in biomechanical behavior between small and large food particle loading becomes highly significant farther posteriorly (Table 3). The results thus support suggestions that posterior molars are poorly designed to dissipate loads resulting from big particles (Table 1), whereas first maxillary molars can cope with a wider range of food particles and loads. While the findings are not unexpected in light of theoretical considerations concerning the functioning of the orofacial skeleton, it needs to be inquired further whether differences in tooth morphology alone could explain the present findings.

Systematic anteroposterior changes in external and internal morphology of maxillary molars were previously reported (e.g., Macho and Moggi Cecchi, 1992; Macho and Berner, 1993, 1994). For example, M^1s have markedly thinner enamel than second and third maxillary molars. While it is evident that the patterning of enamel over the tooth crown influences the patterns of stress distribution within the tooth (Spears and Macho, 1998), its overall thickness may lower the overall magnitudes of tensile stresses (Macho and Berner, 1993; Shellis et al., 1998), i.e., stress is decreased as the enamel shell becomes thicker. Alternatively, enamel thickness may only provide resistance to abrasion, and the thickness of enamel would, in fact, inhibit the dissipation of stress into the tougher dentine (Spears et al., 1993). To test these opposing hypotheses, two simple FESA models were created with identical enamel caps, but different enamel thicknesses (Fig. 3). Tensile stresses were consistently reduced by about 15% when the enamel was thick, irrespective of outer tooth morphology. Hence, an increase in enamel thickness indeed reduces the overall magnitude of tensile stress in that tooth, although this relative improvement cannot be considered substantial. It would thus seem unreasonable to invoke differences in enamel thickness alone to account for differences in overall stress magnitudes between anterior and posterior molars (or between species); other factors, such as abrasion resistance, may be of similar (or even greater) evolutionary importance for determining enamel thickness. Conversely, overall tooth morphology, in particular its cross-sectional geometry, may be a useful tool in assessing the biomechanical behavior of molars in FESA (Khera et al., 1990).

Figure 5 shows a typical first maxillary molar superimposed onto a third maxillary molar, as well as the surface-normal forces which would result from loading a big and small circular food particle at ±30°, respectively. When big circular food particles are loaded, the direction of force is such that the

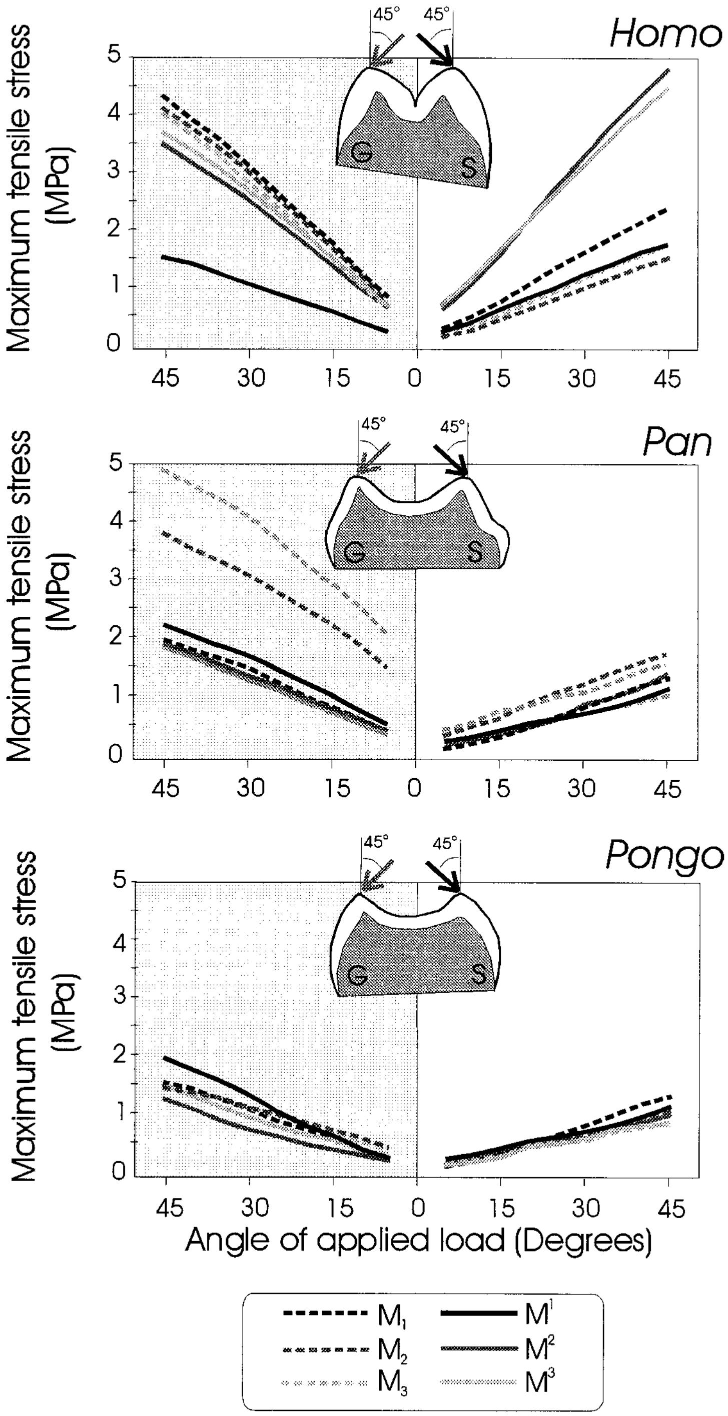

Fig. 4. Maximum values of principal stress when each cusp is subjected to point loads at various angles, for maxillary and mandibular molars separately. For *Homo,* the mean value for each tooth type is shown, whereas for the *Pan* and *Pongo* individuals, results for each tooth are given. S, supporting cusp; G, guiding cusp.

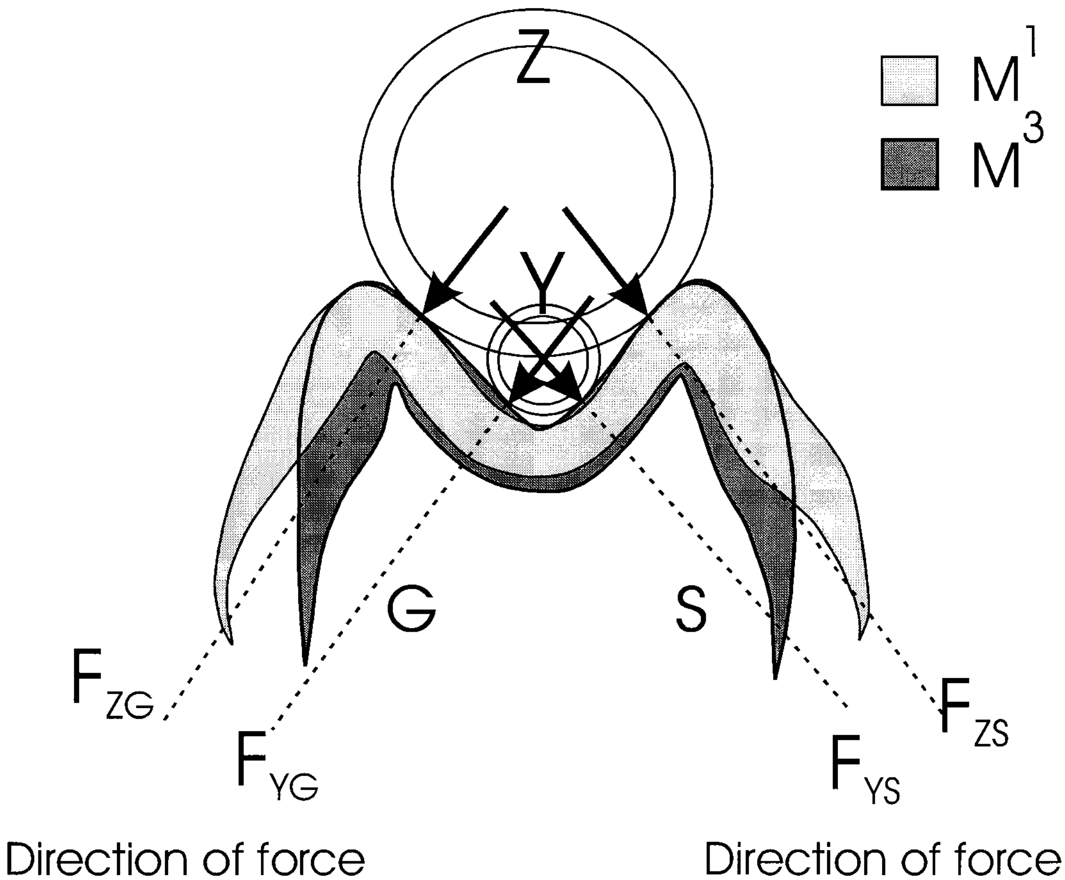

Fig. 5. The direction of force is shown in a typical modern human M^1 and M^3 for small (Y) and big (Z) particle loading at ±30°, respectively. G, guiding cusp; S, supporting cusp.

cusp is unsupported by the bulk of the tooth. This shear component causes outward displacement, which in turn increases the magnitudes of tensile stress in the intercuspal fissure. In M^1s, owing to their wider buccolingual buttresses (Spears and Macho, 1995), forces resulting from loads of either food particle size or direction (F_{ZG}, F_{YG}, F_{YS}, and F_{ZS}) are directed, more or less, into the tooth tissue. Conversely, in M^3 such a situation only occurs when the small food particle is pushed onto the guiding cusp (F_{YG}), and not onto the supporting cusp (F_{YS}); loading of big food particles results in considerable shear components. Cross-sectional geometry of molars thus seem to explain findings of FESA. The bucco-lingual shapes of molars, specifically the extent of their lateral buttresses and the flatness of the occlusal basin, already suggest that human M^1s are likely to be more versatile than M^3s in their function. The structure of the orofacial skeleton, tooth morphology, and the systematic, directional differences in biomechanical behavior between molars in *Homo* all suggest that the masticatory apparatus forms a highly integrated system (Spears and Macho, 1998; this study). Given the overall similarities among hominoid skulls and mastication, it is further reasonable to suggest that great ape molars may differ from those of modern humans only in degree, rather than kind. In part, these predictions are borne out.

The overall stress values obtained for *Pan* molars are much lower than those for *Homo*, implying that chimpanzee molars are well-adapted to resist relatively higher bite forces, as implicated by Demes and Creel (1988).

Buccal, i.e., supporting, cusps of mandibular molars are again stronger than guiding cusps throughout the series, and the differences in biomechanical behavior between the two cusps become especially apparent when big circular food particles are pushed against the teeth (Table 4) or point loads are applied to the cusp tips (Fig. 4). This is comparable to the patterns observed in modern human mandibular molars. However, while all molars (and cusps) of the *Pan* maxilla are equally well-designed to resist loads resulting from small food particles, supporting cusps are generally stronger when large circular food particles are loaded. Cross-sectional geometries of maxillary molars similarly imply that this is the case (Fig. 6). Hence, unlike *Homo*, *Pan* maxillary molars seem relatively unspecialized and may be used as either mortar or pestle. This would accord more closely with the general concept of intercuspating bunodont maxillary and mandibular molars forming a mortar-and-pestle system, with modern human maxillary molars being unique. Alternatively, an explanation can be proffered which implies that *Pan* and *Homo* exhibit similar trends, different only in degree of expression. This proposition is outlined below.

Maximum bite forces on posterior molars can be achieved when the muscles of mastication are optimally stretched; for hominoids this appears at an incisal separation of between 13–28 mm (e.g., Lindauer et al., 1993; Lucas et al., 1994; Paphangkorakit and Osborn, 1997), which would result in a gape of about 10 mm at the level of molars (Lindauer et al., 1993 for modern humans). Microwear studies provide indirect evidence that *Pan* indeed increase the amount of compression from anterior to posterior (Gordon, 1982) which, however, can only be effectively achieved when the food particle is small, i.e., at relatively small gapes. It is thus reasonable to suggest that, although supporting cusps are generally stronger, the results obtained for small food particles more accurately reflect the biomechanical adaptations of maxillary molars in vivo. If correct, the present FESA findings would suggest that maxillary molars are well-designed to resist loads directed at them from different angles and, hence, provide the basin against which the food is pushed by the supporting cusps of mandibular molars. Owing to their less inclined tooth roots and retained anteroposterior disparity in upper and lower dental arch widths (Smith, 1986), lingual cusps of maxillary molars would be expected to be somewhat stronger, despite the occlusal basin forming the “mortar.” Unlike modern humans (Spears and Macho, 1998), near-vertical masticatory loads on posterior maxillary molars in *Pan* would be exerted towards supporting cusps and the occlusal basin. The findings for *Pan* are thus consistent with the specialized mortar-and-pestle system advocated here for maxillary and mandibular molars, respectively. If this interpretation is correct, *Pan* and *Homo* would follow the same general patterns, although the trends in modern humans are exaggerated, probably owing to their complex restructuring of the orofacial skeleton, especially with regard to the retraction of the palate and the inclination of tooth roots. Detailed microwear analyses may provide further clarification (Teaford, 1994). *Pongo*, however, does not seem to follow the same trend.

The overall low maximum stress values obtained are consistent with predictions of maximum bite forces in *Pongo* exceeding those employed here (Lucas et al., 1994) and those of the other hominoids studied. While it would appear that, similar to *Homo* and *Pan*, buccal cusps of mandibular molars are well-suited to act as pestles, results for maxillary molars are less clear-cut. Moreover, both maxillary and mandibular molars are apparently better adapted to dissipate loads on posterior molars, particularly when food particles are large. It should be recognized, however, that the stresses predicted for all *Pongo* molars are reasonably similar and, given the limitations of the FESA models, overinterpretation of the results may not be warranted. Alternatively, the ability of posterior *Pongo* molars to dissipate high loads exerted by large food particles could be related to the unique loss of the anterior belly of the digastric muscle in that species. It has been argued that such muscle loss is advantageous for maintaining, particularly at wide gapes (Wall et al., 1994), a large biting moment. Effective load-dissipation

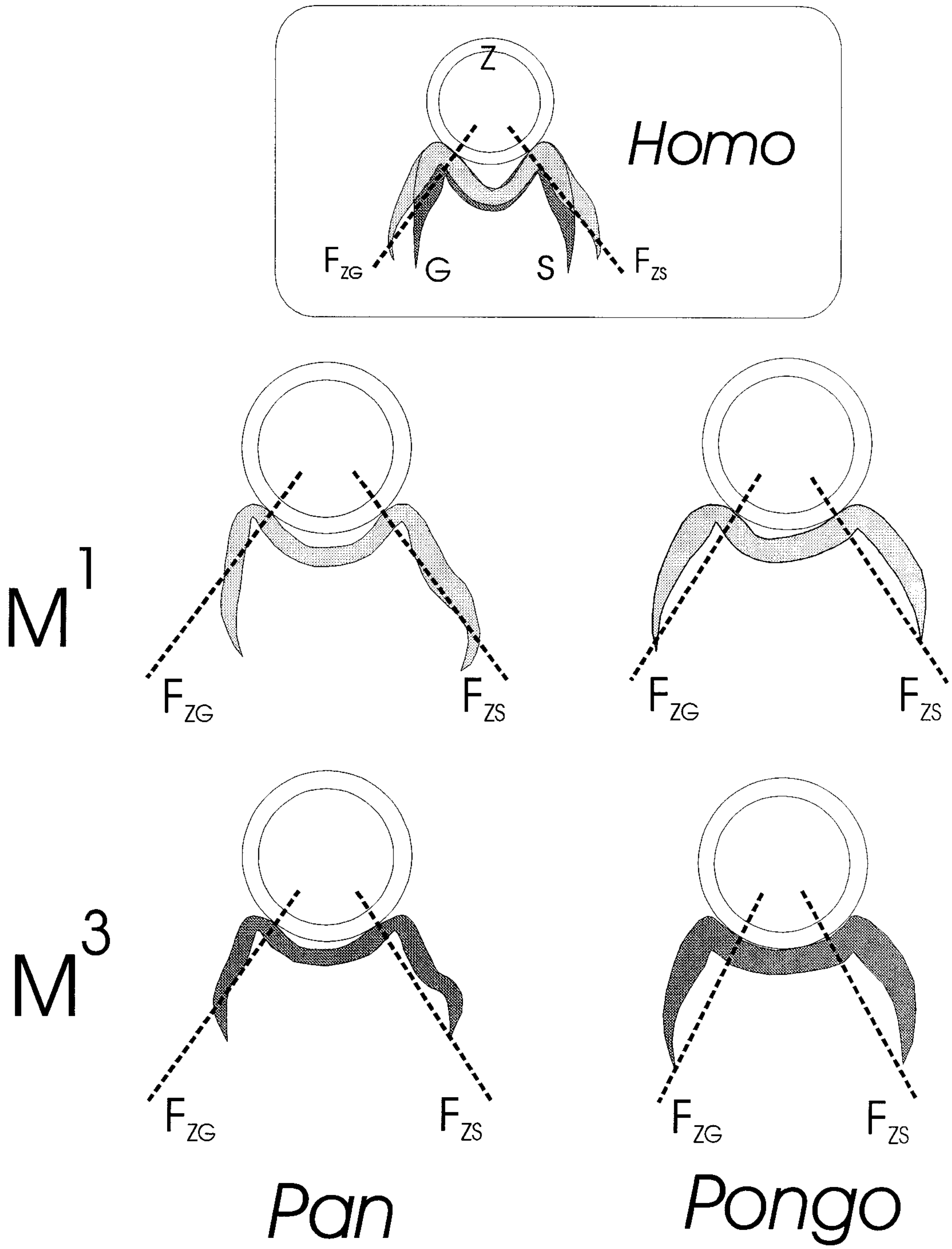

Fig. 6. The direction of force for loading of big particles (Z) is shown for a typical M^1 and M^3, for *Pan* and *Pongo*. S, supporting cusp; G, guiding cusp.

and the ability to maintain high bite forces at wide gape on these most advantageously positioned molars may therefore not be coincidental. It could indicate a very well-adapted masticatory apparatus, in terms of both maximizing durability and minimizing effort, for a diet which often requires breaking into tough and stiff shells.

To conclude, we have attempted to interpret the load-dissipation behavior of molars in terms of what is currently understood about the biomechanics of the primate masticatory apparatus or the species' ecological niche and anatomical specialization. The present findings suggest that the biomechanical behavior of modern human molars is derived, at least with regard to the *Homo/Pan* clade. Conversely, and although the small differences found may be due to the simplifications of the model, trends observed for the molars of *Pongo* could constitute a unique adaptation in that species. Apart from these differences between species, a number of commonalties were found, which may be indicative of the shared evolutionary history of these primates. In particular, the common ability to effectively dissipate loads exerted on some cusps but not on others may imply that the hominoids studied here have adopted a modified mortar-and-pestle arrangement of maxillary and mandibular molars. We thus tentatively conclude that all higher primates, extant and extinct, probably exhibit such a division between upper and lower molars, with maxillary molars resembling a mortar. Further behavioral and experimental, e.g., EMG and FESA, will ultimately clarify some of the issues raised here. Finally, the research design adopted here may prove useful in extracting information from fossil remains, specifically those which preserve relatively complete tooth rows, and in using noninvasive techniques to obtain cross-sectional data on tooth crown profiles.

CONCLUSIONS

1. In hominoids, and perhaps all primates, buccal cusps of mandibular molars are consistently better in load dissipation than lingual cusps; they could be envisaged as pestles.
2. Except for *Homo*, maxillary molars exhibit little difference in biomechanical behavior between lingual and buccal cusps and could act as a "mortar" against which the food is crushed/ground.
3. Overall, maxillary molars appear to be more diverse in their biomechanical behavior among species and seem to reflect differences in the upper facial skeleton more than do mandibular molars.
4. Molars of *Homo* are generally less well-adapted to dissipate loads than are those of *Pan* and *Pongo*; this mirrors data on maximum bite forces and dietary adaptations in these species.
5. *Homo* seems unique in posterior maxillary molars exhibiting more effective load dissipation on guiding cusps, thus appearing relatively stronger than supporting cusps.
6. *Pongo* could be unique in that both mandibular and maxillary molars become increasingly better adapted to dissipate loads posteriorly.
7. Exaggerated increases of enamel thickness by 100% decrease the overall magnitude of maximum tensile stresses only slightly (15%). In contrast, modification to the outer geometry of molars has a more profound effect on load dissipation.

ACKNOWLEDGEMENTS

This work was supported by a grant from the Research Development Fund (Liverpool University) to I.R.S. and the National Environment Research Council (GR9/01635) and the Leverhulme Trust (F/25/BK) to G.A.M. We thank Margit Berner for her help with the sections of modern human maxillary molars, and David Beynon and Chris Dean for making images of human mandibular tooth sections available to us. We are particularly grateful to David Beynon for providing the tooth sections of the *Pan* and *Pongo* specimens. We are grateful to two anonymous reviewers for their constructive comments.

LITERATURE CITED

Andrews P. 1992. Evolution and environment in the Hominoidea. Nature 360:641–646.

Andrews P, Cronin JE. 1982. The relationship of *Sivapithecus* and *Ramapithecus* and the evolution of the orang-utan. Nature 297:541–456.

Asaoka K. 1994. Effects of creep value and occlusal force on marginal adaptation of amalgam filling. J Dent Res 73:1539–1545.

Benefit BR, McCrossin ML. 1997. Earliest known Old World monkey skull. Nature 388:368–371.

Beynon AD, Dean MC, Reid DJ. 1991. Histological study on the chronology of the developing dentition in gorilla and orangutan. Am J Phys Anthropol 86:189–203.

Boesch C, Boesch H. 1990. Tool use and tool making in wild chimpanzees. Folia Primatol (Basel) 54:86–99.

Bowen RL, Rodriguez MS. 1962. Tensile strength and modulus of elasticity of tooth structure and several restorative materials. J Am Dent Assoc 64:378–387.

Delong R, Douglas WH. 1983. Development of an artificial oral environment for the testing of dental restorative: biaxial force and movement control. J Dent Res 62:32–36.

Demes B, Creel N. 1988. Bite force, diet, and cranial morphology of fossil hominids. J Hum Evol 17:657–670.

Fleagle JG. 1988. Primate adaptation and evolution. San Diego: Academic Press. 486 p.

Goel VK, Khera SC, Singh K. 1990. Clinical implications of the response of enamel and dentin to masticatory loads. J Prosthet Dent 64:446–454.

Goel VK, Khera SC, Ralston JL, Chang KH. 1991. Stresses at the dentinoenamel junction of human teeth—a finite element investigation. J Prosthet Dent 66:451–459.

Goel VK, Khera SC, Gurusami S, Chen RCS. 1992. Effect of cavity depth on stresses in a restored tooth. J Prosthet Dent 174:174–183.

Gordon KD. 1982. A study of microwear on chimpanzee molars: implications for dental microwear analysis. Am J Phys Anthropol 59:195–215.

Granath L, Svensson A. 1991. Elastic outward bending of loaded buccal and lingual premolar walls in relation to cavity size and form. Scand J Dent Res 99:1–7.

Holmes DC, Diaz-Arnold AM, Leary JM. 1996. Influence of post dimension on stress distribution in dentin. J Prosthet Dent 73:140–147.

Khera SC, Carpenter CW, Vetter JD, Staley RN. 1990. Anatomy of cusps of posterior teeth and their fracture potential. J Prosthet Dent 64:139–147.

Kim H-S, Takenaka O. 1996. A comparison of TSPY genes from Y-chromosomal DNA of the great apes and humans: sequence, evolution, and phylogeny. Am J Phys Anthropol 100:301–309.

Koolstra JH, van Eijden TMGJ, Weijs WA, Naeije M. 1988. A three-dimensional mathematical model of the human masticatory system predicting maximum possible bite force. J Biomech 21:563–576.

Lee WC, Eakle WS. 1984. Possible role of tensile stress in the etiology of cervical erosive lesions of teeth. J Prosthet Dent 52:374–380.

Lee WC, Eakle W. 1996.. Stress-induced cervical lesions: review of advances in the past 10 years. J Prosthet Dent 75:487–494.

Lindauer SJ, Gay T, Rendell J. 1993. Effect of jaw opening on masticatory EMG-force characteristics. J Dent Res 72:51–55.

Lucas PW, Lowrey TK, Pereira BP, Sarafis V, Kuhn W. 1991. The ecology of *Mezzettia leptopoda* (Hk. f. et Thoms.) Oliv. (Annonaceae) seeds as viewed from a mechanical perspective. Funct Ecol 5:545–553.

Lucas PW, Peters CR, Arrandale SR. 1994. Seed-breaking forces exerted by orangutans with their teeth in captivity and a new technique for estimating forces produced in the wild. Am J Phys Anthropol 94:365–378.

Macho GA, Berner ME. 1993. Enamel thickness of human maxillary molars reconsidered. Am J Phys Anthropol 89:189–200.

Macho GA, Berner ME. 1994. Enamel thickness and the helicoidal occlusal plane. Am J Phys Anthropol 94:327–337.

Macho GA, Moggi Cecchi J. 1992. Reduction of maxillary molars in *Homo sapiens sapiens*: A different perspective. Am J Phys Anthropol 87:151–159.

MacKinnon J. 1971. The orang-utan in Sabah today. Oryx 11:141–191.

MacKinnon J. 1974. The behavior and ecology of wild orang-utans (*Pongo pygmaeus*). Anim Behav 22:3–74.

McGrew WC. 1992.. Chimpanzee material culture. Implications for human evolution. Cambridge: Cambridge University Press. 277 p.

McGrew WC, Marchant LF, Nishida T, editors. 1996. Great ape societies. Cambridge: Cambridge University Press. 328 p.

Meckel AH, Griebstein WJ, Neal RJ. 1965. Structure of mature dental enamel as observed by electron microscopy. Arch Oral Biol 10:775–783.

Mohammad-Ali K, Eladari M-E, Galibert F. 1995. Gorilla and orangutan c-myc nucleotide sequences: inferences on hominoid phylogeny. J Mol Evol 41:262–276.

Moyà Solà S, Köhler M. 1993. Recent discoveries of *Dryopithecus* shed new light on evolution of great apes. Nature 365:543–545.

Osborn JW. 1996. Features of human jaw design which maximize the bite force. J Biomech 29:589–595.

Panitvisai P, Messer HH. 1995. Cuspal deflection in molars in relation to endodontic and restorative procedures. J Endodontol 21:57–61.

Paphangkorakit J, Osborn JW. 1997. Effect of jaw opening on the direction and magnitude of human incisal bite forces. J Dent Res 76:561–567.

Pruim GJ, Ten Bosch JJ, De Hongh HJ. 1978. Jaw muscle EMG-activity and static loading of the mandible. J Biomech 11:389–395.

Rak Y. 1983. The australopithecine face. New York: Academic Press. 169 p.

Rubin C, Krishnamurthy N, Capilouto E, Yi H. 1983. Stress analysis of the human tooth using a three-dimensional finite element model. J Dent Res 62:82–86.

Ruvolo M. 1997. Molecular phylogeny of the hominoids: inferences from multiple independent DNA sequence data sets. Mol Biol Evol 14:248–265.

Sakaguchi RL, Cross M, Brust E, Delong R, Douglas WH. 1991. Independent movement of cusps during occlusal loading. Dent Mat 7:186–190.

Sakaguchi RL, Cross M, Douglas WH. 1992. A simple model of crack propagation in dental restorations. Dent Mat 8:131–136.

Shellis RP, Beynon AD, Reid DJ, Hiiemae KM. 1998. Variations in molar enamel thickness among primates. J Hum Evol 35:507–522.

Smith BH. 1986. Development and evolution of the helicoidal plane of dental occlusion. Am J Phys Anthropol 69:21–35.

Spears IR. 1994. Functional adaptations of hominoid molars: an engineering approach. Unpublished Ph.D. dissertation, University of Liverpool.

Spears IR. 1997. A three-dimensional finite element model of prismatic enamel: a reappraisal of the data on the Young's modulus of enamel. J Dent Res 76:1690–1697.

Spears IR, Macho GA. 1995. The helicoidal occlusal plane—a functional and biomechanical appraisal of molars. In: Radlanski RJ, Renz H, editors. Proceedings of the 10th International Symposium on Dental Morphology. Berlin: "M" Marketing Services C. & M. Brünne GbR. p 391–297.

Spears IR, Macho GA. 1998. Biomechanical behavior of modern human molars: implications for interpreting the fossil record. Am J Phys Anthropol 106:467–482.

Spears IR, van Noort R, Crompton RH, Cardew GE, Howard IC. 1993. The effects of enamel anisotropy on the distribution of stress in a tooth. J Dent Res 72:1526–1531.

Teaford MF. 1994. Dental microwear and dental function. Evol Anthropol 3:17–30.

Wall CE, Larson SG, Stern JT. 1994. EMG of the digastric muscle in gibbon and orangutan: functional consequences of the loss of the anterior digastric in orangutans. Am J Phys Anthropol 94:549–567.

Waters NE. 1980. Some mechanical and physical properties of teeth. In: Vincent JFV, Curry JD, editors. The mechanical properties of biological materials. Cambridge: Cambridge University Press. p 99–135.

Yettram AL, Wright KWJ, Pickard HM. 1976. Finite element stress analysis of the crowns of normal and restored teeth. J Dent Res 55:1004–1011.